^{87}Rb NMR study of the paraelectric-antiferroelectric phase transition in $Rb_{0.22}(ND_4)_{0.78}D_2PO_4$

R. Kind, O. Liechti, and R. Brüschweiler
Eidgenössische Technische Hochschule Zürich–Hönggerberg, Laboratorium für Festkörperphysik, Zürich, Switzerland

J. Dolinšek and R. Blinc
J. Stefan Institute, E. Kardelj University of Ljubljana, Ljubljana, Yugoslavia
(Received 15 January 1987)

^{87}Rb $\frac{1}{2}\rightarrow-\frac{1}{2}$ NMR line-shape and spin-lattice relaxation data demonstrate the presence of a first-order phase transition from a paraelectric (PE) to an antiferroelectric (AFE) phase for the mixed crystal $Rb_{0.22}(ND_4)_{0.78}D_2PO_4$ around $T_c=150$ K. The transition is driven by an antiferroelectric soft mode as in pure $NH_4H_2PO_4$. Between 150 and 140 K the PE and the AFE phases overlap, and a continuous decrease of the paraelectric volume fraction or an increase of the antiferroelectric one, respectively, was observed. The determination of the ^{87}Rb electric-field-gradient (EFG) tensors in both phases revealed that the average symmetry relations of the EFG tensors are consistent with the space groups $I\bar{4}2d$ (PE phase) and $P2_12_12_1$ (AFE phase), respectively, of the pure $NH_4H_2PO_4$ crystal. The increase in the inhomogeneous broadening of the NMR lines with decreasing temperature indicates an incipient glassy-type ordering before the AFE long-range ordering sets in.

I. INTRODUCTION

Substitutionally disordered mixed crystals $Rb_{1-x}(NH_4)_xH_2PO_4$—henceforth designated as RADP—of ferroelectric RbH_2PO_4 (RDP) and antiferroelectric $NH_4H_2PO_4$ (ADP) represent a frustrated H-bonded system[1,2] with random competing ferroelectric and antiferroelectric interactions. The system shows for small x a paraelectric-ferroelectric transition and for large x a paraelectric-antiferroelectric transition whereas no long-range structural ordering takes place for $0.22\leq x\leq 0.75$ and the system forms at low temperatures a "proton" or "deuteron" glass.

Very recently it has been shown[3–5] that the situation may be more complicated than assumed so far. On the anitferroelectric side of the phase diagram both a glasslike dielectric dispersion anomaly at low temperatures and an antiferroelectric dielectric anomaly at somewhat higher temperatures were observed for $0.7\leq x\leq 0.8$, indicating the possible existence of a reentrant glassy phase.[3,5] For $x=0.7$ and 0.74 the structure is tetragonal above and below the dielectric constant and hidden heat capacity[4] anomaly. For $x=0.8$ and 0.89 the two anomalies in the dielectric constant and heat capacity are well developed. The structure of the low-temperature phase is here orthorhombic as in antiferroelectric $NH_4H_2PO_4$ while the structure of the intermediate phase is still unknown. Two kinds of dielectric dispersions have been also observed on the ferroelectric side of the phase diagram[5] in the range $0.15\leq x\leq 0.25$.

In order to throw some additional light on the nature of these transitions and the local ordering[6] at the antiferroelectric side of the phase diagram we decided to perform a ^{87}Rb NMR study of the $Rb_{0.22}(ND_4)_{0.78}D_2PO_4$ system. We particularly hoped to determine the electric-field-gradient (EFG) tensors at the ^{87}Rb sites—which substitute for the NH_4^+ ions—and find out the effect of randomness of this substitution on the distribution of EFG tensors around their average values. We also wanted to see if the O—D $\cdots$ O dynamics is of the "glassy" type[7] or determined by a soft mode as in pure ADP and RbDP.[8]

II. EXPERIMENT

The experiments were performed on a RADP crystal with an ammonium concentration $x=0.78$ as determined by flame spectroscopy and a deuteration content of about 90%. The ^{87}Rb $\frac{1}{2}\rightarrow\frac{1}{2}$ NMR spectra were measured in a field of 7 T and the spin-lattice relaxation time in a field of 6.3 T. A Fourier transform $(90°)_x-(90°)_y$ solid echo technique was used. The homogeneous linewidth was determined from the slope of the spin-echo amplitude versus pulse-separation plot.

III. RESULTS

A. Temperature dependence of the NMR line shape and observation of the phase transition to the antiferroelectric phase

The effect of substitutional disorder and the resulting static EFG-tensor distribution leads to an inhomogeneous broadening of the ^{87}Rb nuclear-quadrupole-resonance (NQR) lines. In all RADP mixed crystals this broadening is so large that a direct observation of the pure NQR lines becomes impossible. Even the $+\frac{1}{2}\leftrightarrow-\frac{1}{2}$ transition in a magnetic field of 2 T could not be observed for most of the crystal orientations in the case of

$Rb_{0.65}(NH_4)_{0.35}H_2PO_4$.[7] In a magnetic field of 7 T, however, it was possible to obtain the full rotation pattern of the central line for a single crystal of $Rb_{0.22}(ND_4)_{0.78}D_2PO_4$ (D-RADP-78) at room temperature (Fig. 1). The inhomogeneous linewidth is strongly orientation dependent and becomes as high as 20 kHz at room temperature, whereas the homogeneous linewidth is only 300 Hz. Here the crystal was rotated around the crystallographic a axis. For $\beta=0$ the magnetic field $\mathbf{B}_0$ is parallel to the c axis of the crystal. In agreement with the average site symmetry of the paraelectric phase $\bar{4}2m$ there is just a single line in the rotation spectrum and $\bar{\nu}_Q=3.501$ MHz, $\bar{\eta}=0$, $\bar{\alpha}=0$, $\bar{\beta}_0=0$, $\bar{\gamma}=0$, i.e., the Rb EFG tensor is axially symmetric and the principal axes (X,Y,Z) are parallel to the crystal axes (x,y,z).

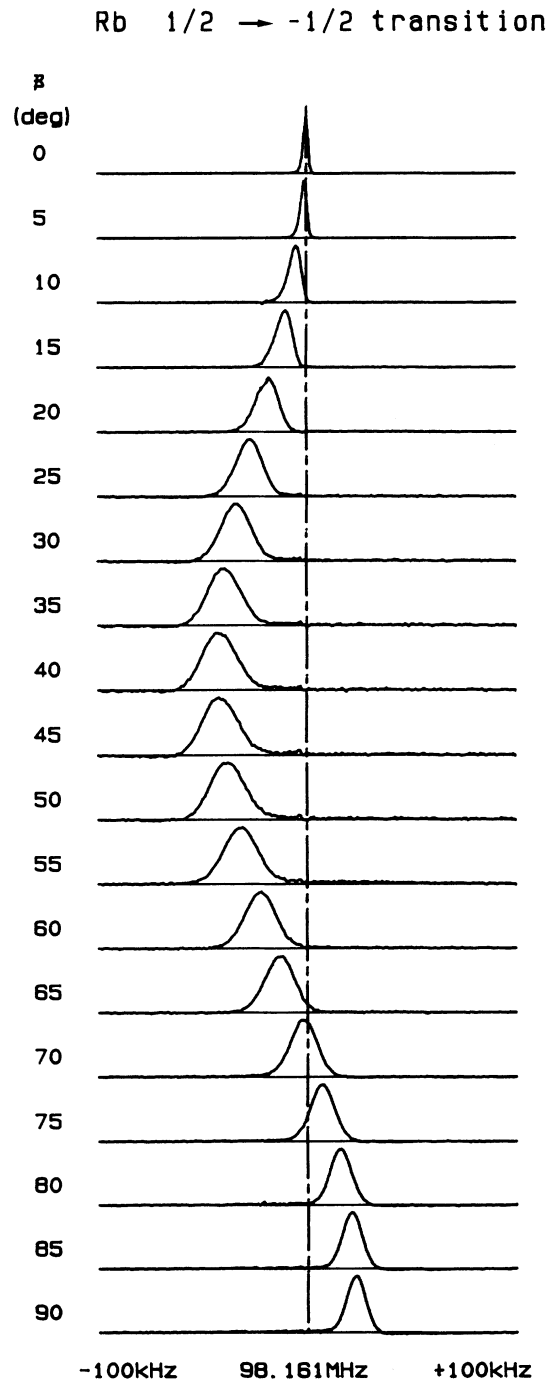

FIG. 1. Orientation dependence of the ^{87}Rb $\frac{1}{2}\rightarrow-\frac{1}{2}$ NMR spectra of D-RADP-78 at $T=296$ K ($\mathbf{a}\perp\mathbf{B}_0$, $\beta=0$, for $\mathbf{c}\|\mathbf{B}_0$).

On lowering the temperature, $\bar{\nu}_Q$ steadily decreases and reaches 3.2 MHz at 149 K. The NMR lines continuously broaden from room temperature down to 150 K, where the first signs of the phase transition become visible. The maximum linewidth in the rotation pattern reaches now 30 kHz. The orientation dependence of the ^{87}Rb NMR linewidth at 155 K is presented in Fig. 2.

Figure 3 shows the temperature dependence of the NMR signal for $\beta=0$ (i.e., for $\mathbf{B}_0\|\mathbf{c}$) in a temperature range 152–143 K. About 35 kHz below the paraelectric line a new broad line grows out of the noise and coexists with the paraelectric line down to 140 K where the paraelectric line disappears. Thus, the second line belongs to the low temperature phase. Within the time scale of our measurements (hours) we did not observe any sign of a time dependence of the relative intensities of the two lines and no significant thermal hysteresis could be found. In Fig. 4 the relative intensities [i.e., the volume fractions of the paraelectric (PE) and antiferroelectric (AFE) phases] are plotted versus temperature. At 148 K the two volume fractions are approximately equal.

In Fig. 5 the Rb NMR spectrum at 135 K is plotted as a function of the rotation angle β. Up to four different lines can be distinguished now. The maxima of these lines give rise to the rotation pattern shown in Fig. 6. The four solid lines are the calculated rotation patterns fitted to the data points. They correspond to four different average ^{87}Rb EFG tensors which are related by the symmetry operation $42m$. This symmetry is still the

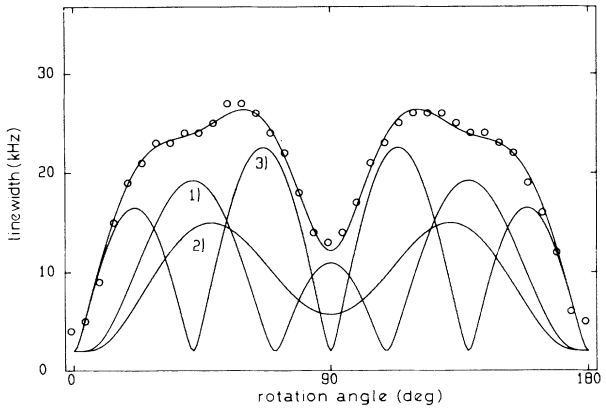

FIG. 2. Orientation dependence of the inhomogeneous linewidth of the ^{87}Rb $\frac{1}{2}\rightarrow-\frac{1}{2}$ NMR spectra at $T=155$ K. ($\mathbf{a}\perp\mathbf{B}_0$, $\beta=0$ for $\mathbf{c}\|\mathbf{B}_0$). The solid line is the theoretical curve according to Eq. (9) and (8). Curve (1) designates the σ_{ν_Q}, curve (2) the σ_η, and curve (3) the σ_{β_0} contribution.

full symmetry of the paraelectric phase but the general orientation of the four EFG tensors with respect to the crystal axes indicates that the site symmetry $\bar{4}$ is lost at the Rb sites. Moreover, it indicates that the two glide mirror planes d_a and d_b are lost in the low-temperature unit cell since they generate a twofold axis 2_z at the Rb site, which would fix one EFG-tensor axis to the c direction of the crystal, as it is the case in the ferroelectric phase of RDP.[8] The remaining symmetry elements are, thus, $2_{1x}2_{1y}2_{1z}$, in agreement with the space group $P2_12_12_1$ of the antiferroelectric phase of ADP. The higher apparent symmetry between the mean EFG tensors indicates, thus, the presence of antiferroelectric 90° domains, according to the well-known fact that domains occurring at the low-temperature side of a distortive phase transition are related by the lost symmetry elements of the parent phase.

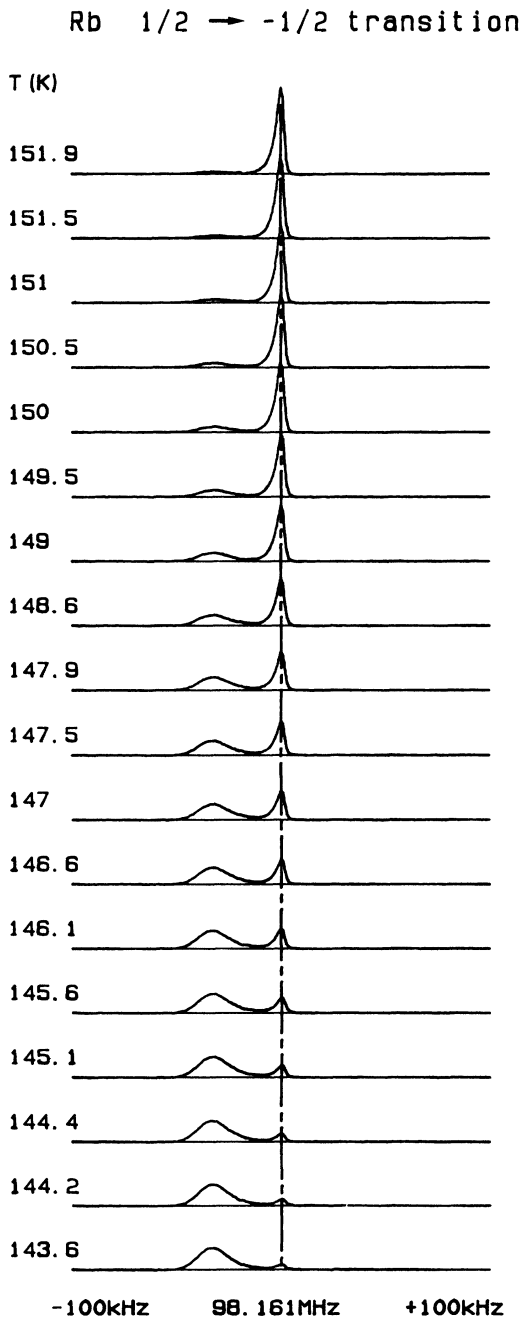

FIG. 3. Temperature dependence of the ^{87}Rb $\frac{1}{2}\rightarrow-\frac{1}{2}$ NMR spectra in the region of the paraelectric-antiferroelectric phase transition for $\mathbf{c}\|\mathbf{B}_0$.

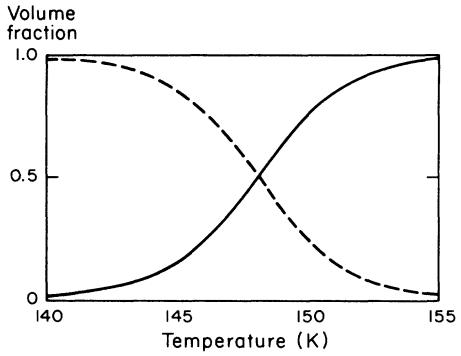

FIG. 4. Volume fractions of the paraelectric (solid line) and antiferroelectric phase (dashed line) of D-RADP-78 as functions of temperature.

The four average EFG tensors are given by $\nu_Q=4.180$ MHz, $\bar{\eta}=0.23$, and

$$\alpha_1=-19°,\ \beta_{01}=-12°,\ \gamma_1=-10°,$$
$$\alpha_2=19°,\ \beta_{02}=-12°,\ \gamma_2=-10°,$$
$$\alpha_3=-12°,\ \beta_{03}=-19°,\ \gamma_3=84°,$$
$$\alpha_4=-12°,\ \beta_{04}=-19°,\ \gamma_4=84°,$$

i.e., they are fully determined in terms of the tetragonal crystal coordinates[9] but it is not possible to assign the two sets (1,2) or (3,4) respectively, to the individual 90° domains. The average tilt angle of the principal Z axes with respect to the c axis of the crystal is 22.4° for all four tensors.

The above results agree with a recent extended x-ray-absorption fine-structure (EXAFS) study[6] of the radial distribution function around the Rb atom, which showed that for $x=0.3$ and 0.5 the local surrounding of the Rb ion is of the RbH_2PO_4 type and, for $x=0.7$, of the $NH_4H_2PO_4$ type.

B. Temperature dependence of the ^{87}Rb spin-lattice relaxation time

Whereas the NMR line shape reflects the effects of static disorder, and the increase in the inhomogeneous linewidth with decreasing temperature shows the onset of a glassy-type short-range ordering before the transition into the AFE phase, the spin-lattice relaxation rate reveals the dynamics of the transition.

The temperature dependence of the ^{87}Rb $\frac{1}{2} \rightarrow -\frac{1}{2}$ spin-lattice relaxation time T_1 is shown in Fig. 7 for $\mathbf{c} \| \mathbf{B}_0$, $\mathbf{a} \perp \mathbf{B}_0$, and $\nu_L = 88.346$ MHz. From room temperature down to $T_c = 150$ K, T_1 slowly decreases from 40 to about 7.5 ms. At T_c it discontinuously increases from 7.5 to about 600 ms and then gradually increases with decreasing temperature. The observed temperature dependence of T_1 at $x = 0.78$ is thus completely different from the one found in RADP with $x = 0.35$ (Ref. 7) and deuterated RADP with $x = 0.55$.[10] These two substances remain in an incipient glassy state in the whole investigated temperature range and show a broad asymmetric minimum in the $\ln T_1$ versus $10^3/T$ plot.

Measurements in deuterated and undeuterated samples[7,10] have shown that the Rb spin-lattice relaxation rate is determined by the deuteron and proton motion, respec-

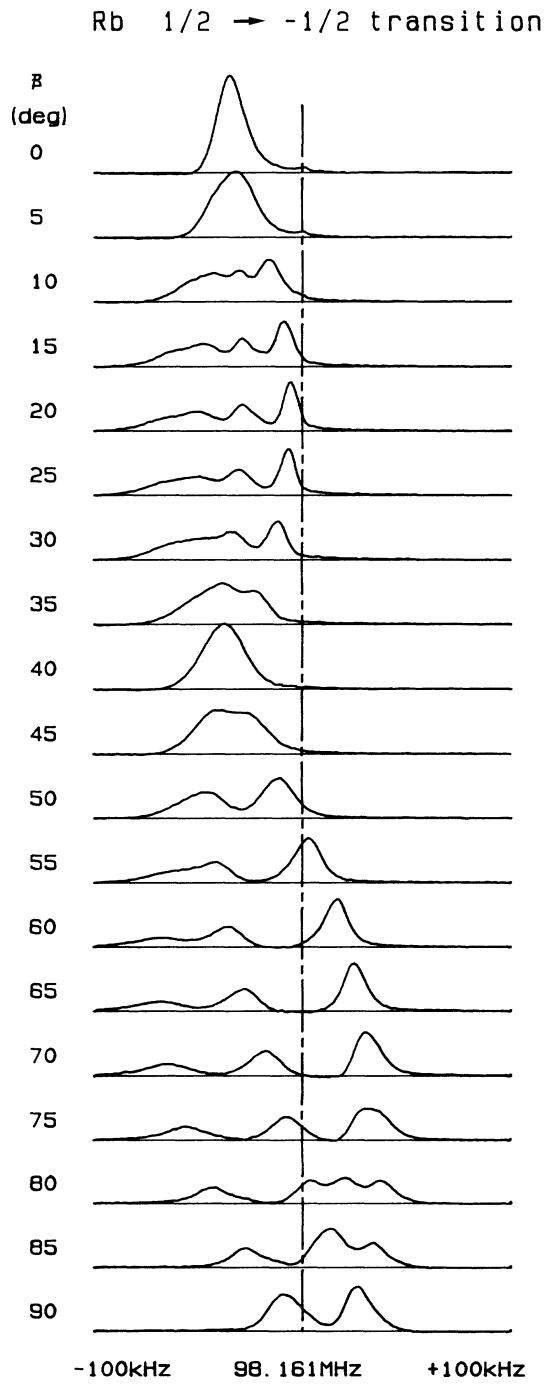

FIG. 5. Orientation dependence of the ^{87}Rb $\frac{1}{2} \rightarrow -\frac{1}{2}$ NMR spectra of D-RADP-78 at $T = 135$ K ($\mathbf{a} \perp \mathbf{B}_0$, $\beta = 0$ for $\mathbf{c} \| \mathbf{B}_0$).

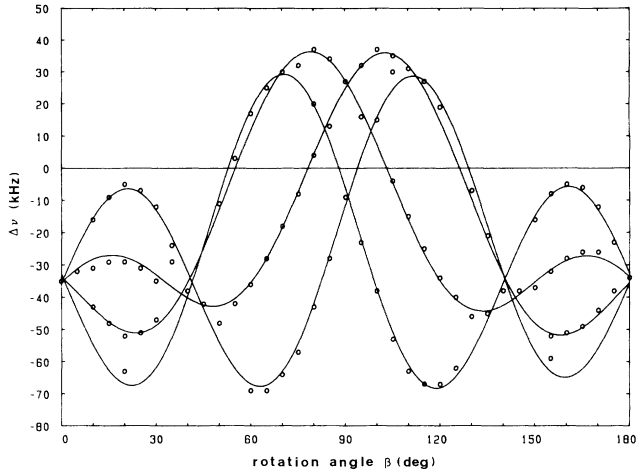

FIG. 6. Angular dependence of the $\frac{1}{2} \rightarrow -\frac{1}{2}$ ^{87}Rb NMR transition frequencies in D-RADP-78 at $T = 135$ K. The solid lines are the theoretical curves.

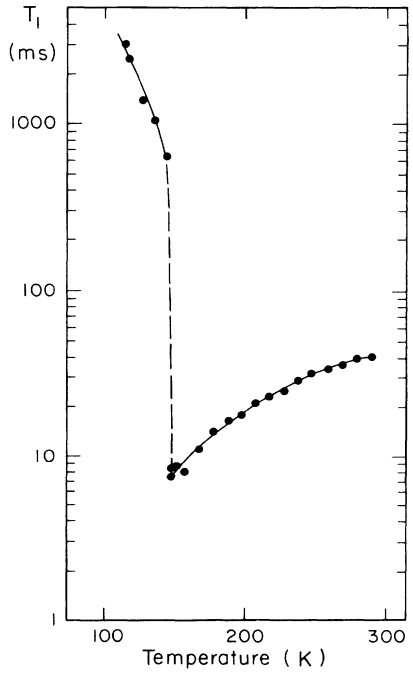

FIG. 7. Temperature dependence of the ^{87}Rb $\frac{1}{2} \rightarrow -\frac{1}{2}$ spin-lattice relaxation time in D-RADP-78.

tively, between the two equilibrium sites in the O—H · · · O bonds. The absence of a Rb T_1 minimum in RADP with $x=0.78$ thus demonstrates that the dynamics of the O—D · · · O bonds—which represent the main reversible electric dipoles in the structure—is completely different from the one observed in "glassy" systems[7,10] with $x=0.35$ and 0.55. The shape of the observed T_1 anomaly suggests that T_1 is determined by an antiferroelectric soft mode of the ADP type,[11] similar to the manner in which the Rb T_1 in pure RDP is determined by the ferroelectric soft mode.[8]

IV. DISCUSSION

A. Distribution and average symmetry properties of the EFG tensor at the Rb site

The main difference between pure compounds of the KH_2PO_4 family and substitutionally disordered systems is that in addition to the dynamic disorder (deuteron hopping between equivalent sites in the O—D · · · O bonds) there is also a static spatial disorder present in the latter case. As a consequence, the site symmetry given by the space group of the pure system is broken for the individual sites in the mixed crystal RADP. This leads to a random distribution of EFG tensors at the Rb sites[6] in RADP.

X-ray and EXAFS measurements of RADP (Refs. 1, 2, and 6) have shown that the structural disorder is weak so that the space-averaged space group $I\bar{4}2d$ of the parent paraelectric phase is maintained. The site symmetry of the Rb is $\bar{4}$ in this space group and the two Rb sites in the primitive unit cell are chemically equivalent. Thus, the space-averaged Rb EFG tensor in RADP should be axially symmetric with its z axis parallel to c. This is in fact the case.

The question now is: What does the distribution of EFG tensors around the space-averaged value look like? The answer depends on the nature of the probe, i.e., of the nucleus or atom under consideration. In case of strong covalent bonding the nucleus probes only the local surrounding, i.e., one can expect a random distribution between a few distinct EFG tensors, i.e., a discrete distribution. This would lead to a set of distinct resonance lines. In case of ionic bonding, however (as e.g., for Rb in RADP), the EFG tensor is nonlocal and is influenced also by charges which are several lattice constants away, i.e., one has to expect a continuous (i.e., Gaussian) distribution around the average EFG tensor.

The EFG tensor at the Rb sites in paraelectric RDP is diagonal in the crystal fixed frame. The same should be true for isostructural paraelectric ADP in the absence of substitutional disorder. We therefore assume Gaussian distributions of the five EFG-tensor elements around the average tensor elements of the mean Rb EFG tensor of RADP in its *diagonal form*. The mean EFG tensor can now be expressed as

$$\bar{V}=\frac{\overline{eq}}{2}\begin{pmatrix}1-\bar{\eta} & 0 & 0\\ 0 & 1+\bar{\eta} & 0\\ 0 & 0 & -2\end{pmatrix}, \tag{1}$$

where $\overline{eq}\equiv\overline{V_{ZZ}}$ is the average EFG strength and $\bar{\eta}$ the average asymmetry parameter. The Gaussian distributions are given by the following expressions:

$$\begin{aligned} &p(eq)\propto \exp[-(eq-\overline{eq})^2/2\sigma_{eq}^2]\ ,\\ &p(\eta)\propto \exp[-(\eta-\bar{\eta})^2/2\sigma_{\eta}^2]\ ,\\ &p(v_{jk})\propto \exp[-(v_{jk}^2)/2\sigma_{jk}^2]\quad (j\neq k)\ , \end{aligned} \tag{2}$$

where $v_{jk}=2V_{jk}/\overline{V_{ZZ}}$.

In order to visualize the meaning of the v_{jk} (e.g., v_{yz}) we perform a rotation of the mean EFG tensor around the x axis by the angle θ_x,

$$\bar{V}'=\frac{\overline{eq}}{2}\begin{pmatrix}1-\bar{\eta} & 0 & 0\\ 0 & (3+\bar{\eta})\cos^2\theta_x-2 & \frac{3}{2}(1+\bar{\eta})\sin 2\theta_x\\ 0 & \frac{3}{2}(1+\bar{\eta})\sin 2\theta_x & (3+\bar{\eta})\sin^2\theta_x-2\end{pmatrix}. \tag{3}$$

Assuming that the angle θ_x is small we can write

$$\bar{V}'\approx\frac{\overline{eq}}{2}\begin{pmatrix}1-\bar{\eta} & 0 & 0\\ 0 & 1+\bar{\eta} & 3(1+\bar{\eta})\theta_x\\ 0 & 3(1+\bar{\eta})\theta_x & -2\end{pmatrix} \tag{4}$$

and we get $v_{yz}\approx 3(1+\bar{\eta})\theta_x$. The Gaussian distribution of v_{yz} corresponds thus to a Gaussian distribution of the tilt angle θ_x of the EFG-tensor axes Z and Y about the X axis around their average orientations.

Similarly, we obtain $v_{xz}\approx 3(1-\bar{\eta})\theta_y$ and $v_{xy}\approx 2\bar{\eta}\theta_z$ and their distributions correspond to the distribution of the tilt angles around the Y and Z axes, respectively.

So far we have just analyzed cases where only one of the five elements differs from the average value. In general, all elements differ from the average values for a given Rb position, but one can show that this leads only to second-order correction terms in the v_{ik}, which can be safely neglected for small θ_i. A special case is the term v_{xy} for $\bar{\eta}=0$. It consists of a sum of second-order terms, as, e.g., $2\eta\theta_z$, $3\theta_x\theta_y$, etc., and its distribution is different from Gaussian, but this is of minor importance.

To conclude this section one can say that we are left with Gaussian distributions $p(eq)$, $p(\eta)$, $p(\theta_x)$, $p(\theta_y)$, and $p(\theta_z)$, if only the linear terms are of importance. The corresponding Gaussian half-widths are σ_{eq}, σ_η, σ_x, σ_y, and σ_z. For the tetragonal phase of RADP we have, for symmetry reasons, $\bar{\eta}=0$, $\sigma_x=\sigma_y$, and $\sigma_z=0$.

B. Influence of the EFG-tensor distribution on the ^{87}Rb NMR line shape

In order to analyze the influence of the EFG tensor distribution on the angular dependence of the linewidth, we have to relate the distributions obtained in Sec. IV A with the parameters used to calculate the second-order-shift rotation pattern for a spin $\frac{3}{2}$. The second-order shift is given by

$$\Delta\nu = -\frac{1}{12}\frac{\nu_Q^2}{\nu_L}\{\tfrac{9}{4}(1-c^2)(9c^2-1) + \eta[-\tfrac{3}{2}(a^2-b^2)(9c^2+1)] + \eta^2[2-3c^2-\tfrac{9}{4}(a^2-b^2)^2]\}\ , \quad (5)$$

where ν_L is the Larmor frequency, $\nu_Q = e^2qQ/2h$, and a, b, c are the direction cosines of the magnetic field vector $\mathbf{B}_0$ with respect to the principal EFG-tensor axes X, Y, Z. These direction cosines are given by

$$\begin{aligned} a &= -\sin\gamma\sin\alpha\cos(\beta-\beta_0) - \cos\gamma\sin(\beta-\beta_0)\ , \\ b &= \cos\gamma\sin\alpha\cos(\beta-\beta_0) - \sin\gamma\sin(\beta-\beta_0)\ , \\ c &= \cos\alpha\cos(\beta-\beta_0)\ , \end{aligned} \quad (6)$$

in contrast to the usual definition in polar coordinates (θ,ϕ). Equations (6) takes care of the fact that the magnetic field vector $\mathbf{B}_0$ moves in a plane during the crystal rotation in any arbitrarily oriented frame of EFG-tensor axes. This plane of $\mathbf{B}_0$ motion is defined in a given EFG-tensor frame by the angles α (tilt angle of the $\mathbf{B}_0$ plane with respect to the Z axis) and γ (angle between the X axis and the intersection line of the $\mathbf{B}_0$ plane with the XY plane). The angle $\beta-\beta_0$ defines the actual orientation of $\mathbf{B}_0$ within the plane, β is the running angle, and β_0 defines the zero position which is usually chosen in the ab plane of the crystal so that the EFG tensor is determined completely in terms of crystal coordinates. For more details see Ref. 9.

For our rotation pattern in Fig. 1, we have $\bar{\alpha}=0$, $\bar{\beta}_0=0$, $\bar{\gamma}=0$, and $\bar{\eta}=0$. For this case we have the relations $\alpha=-\theta_x$, $\beta_0=\theta_y$, and $\gamma=-\theta_z$ and thus the corresponding distributions have a one-to-one relation.

For an individual EFG tensor with given deviations $\delta\nu_Q$, $\delta\eta$, $\delta\alpha$, $\delta\beta_0$, and $\delta\gamma$ from the mean values, one can expand Eq. (5) around the mean value $\overline{\Delta\nu}$ by taking the partial first derivatives of Eq. (5) with respect to the δ_i:

$$\overline{\Delta\nu}+\delta\nu = \overline{\Delta\nu} + \frac{\partial\Delta\nu}{\partial\nu_Q}\delta\nu_Q + \frac{\partial\Delta\nu}{\partial\eta}\delta\eta + \frac{\partial\Delta\nu}{\partial\alpha}\delta\alpha + \frac{\partial\Delta\nu}{\partial\beta_0}\delta\beta_0 + \frac{\partial\Delta\nu}{\partial\gamma}\delta\gamma\ , \quad (7)$$

$$\begin{aligned} \frac{\partial\Delta\nu}{\partial\nu_Q}\delta\nu_Q &= \frac{3}{8}\frac{\nu_Q}{\nu_L}(9\cos^4\beta - 10\cos^2\beta + 1)\delta\nu_Q\ , \\ \frac{\partial\Delta\nu}{\partial\eta}\delta\eta &= \frac{1}{8}\frac{\nu_Q^2}{\nu_L}(\tfrac{9}{4}\sin^2 2\beta + \sin^2\beta)\delta\eta\ , \\ \frac{\partial\Delta\nu}{\partial\beta_0}\delta\beta_0 &= \frac{3}{8}\frac{\nu_Q^2}{\nu_L}[(5-9\cos^2\beta)\sin 2\beta]\delta\beta_0\ , \\ \frac{\partial\Delta\nu}{\partial\alpha} &= \frac{\partial\Delta\nu}{\partial\gamma} = 0\ , \end{aligned} \quad (8)$$

for $\bar{\alpha}$, $\bar{\beta}_0$, $\bar{\gamma}$, $\bar{\eta}=0$.

From this one can see that only the distributions $p(\nu_Q)$, $p(\eta)$, and $p(\beta_0)$ affect the line shape in first order. The angular dependences of the Gaussian half-widths $\sigma(\delta\nu_i)$ are given by Eqs. (8) by replacing the δ_i by the σ_i. The total lineshape is then given by the convolution of the Gaussian line shapes $p(\delta\nu_i)$. Since the convolution of two Gaussians with linewidths σ_a and σ_b is again a Gaussian with linewidth $\sigma_{ab}=(\sigma_a^2+\sigma_b^2)^{1/2}$, the resulting lineshape is again a Gaussian which is centered at $\overline{\Delta\nu}$. Thus, the observed resonance lines should be symmetric as long as only linear effects are of importance. As one can see in Fig. 1 the lines are fairly symmetric except close to $\beta=0$ where the linear terms vanish and the lineshape is determined by the homogeneous line and inhomogeneous second-order contributions.

Using the relation

$$\sigma_{\text{tot}} = \left[\sum_i \sigma^2(\delta\nu_i)\right]^{1/2}\ , \quad (9)$$

one can obtain the values of σ_{ν_q}, σ_η, and σ_{β_0} by a fit of Eqs. (8) and (9) to the measured orientation dependence of the NMR linewidth as shown in Fig. 2. The room-temperature data obtained from Figs. 1 and 2 are $\nu_Q=3.501$ MHz, $\bar{\eta}=0$, $\sigma_{\nu_Q}=307$ kHz, $\sigma_\eta=0.09$, and $\sigma_{\beta_0}=\sigma_x=\sigma_y=2.2°$. The high value of σ_{ν_Q} clearly shows why a direct observation of the NQR line or the NMR satellites is not possible. At 149 K we have $\nu_Q=3.20$ MHz, $\bar{\eta}=0$, $\sigma_{\nu_Q}=375$ kHz, $\sigma_\eta=0.12$, and $\sigma_{\beta_0}=4.4°$. The relative increase with respect to the room-temperature values is 1.2 for σ_{ν_Q} and σ_η, but 2.0 for σ_{β_0}. Thus, the main contribution to the line broadening comes from the distribution in tilt angles $p(\theta_x)=p(\theta_y)$.

V. CONCLUSIONS

The ^{87}Rb NMR line-shape and T_1 data demonstrate the occurrence of a first-order phase transition in RADP with $x=0.78$ at $T_c=148$ K. The average symmetry of the Rb EFG tensors—deduced from the angular dependence of the NMR frequencies—is consistent with the $I\bar{4}2d$ space group for the high-T and the $P2_12_12_1$ space group for the low-T phase, thus demonstrating that we are dealing with a paraelectric-antiferroelectric transition as in pure ADP. The two phases overlap in a region of about 10 K. The distributions of the EFG tensors around their mean values have been deduced from the angular dependence of the Rb linewidths. They show the presence of a glassy-type static disorder which becomes more prominent at lower temperatures.

Superimposed on the static glassy-type disorder is a dynamic disorder of the deuterons in the O—D $\cdots$ O bonds. This disorder is driven by a an antiferroelectric soft mode which determines the Rb T_1 and freezes out at T_c. The freeze-out of the antiferroelectric soft mode results in long-range ordering of the AFE type.

Our experiments did not reveal any sign of an intermediate incommensurate phase, though incommensurate short-range order extending over one or two unit cells cannot be ruled out.

[1]E. Courtens, Jpn. J. Appl. Phys. **24**, 70 (1985), Suppl. 24-2 and references therein.
[2]H. A. Terauchi, Jpn. J. Appl. Phys. **24**, 75 (1985), Suppl 24-2 and references therein.
[3]M. Takashige, H. Terauchi, Y. Mora, and S. Hoshino, J. Phys. Soc. Jpn. **54**, 3250 (1985).
[4]K. Moriya, T. Matsuo, H. Suga, and H. Terauchi, Jpn. J. Appl. Phys. **24**, 956 (1985), Suppl. 24-2.
[5]M. Takashige, H. Terauchi, Y. Miura, S. Hoshino, and T. Nakamura, Jpn. J. Appl. Phys. **24**, 947 (1985), Suppl. 24-2.
[6]Y. Nishihata, H. Sakashita, and H. Terauchi, Jpn. J. Appl. Phys. **24**, 961 (1985), Suppl. 24-2.
[7]J. Slak, R. Kind, R. Blinc, E. Courtens, and S. Žumer, Phys. Rev. B **30**, 85 (1984).
[8]R. Blinc, M. Mali, and S. Žumer, J. Chem. Phys. **63**, 2898 (1975).
[9]R. Kind, Z. Naturforsch. **41A**, 122 (1986).
[10]R. Blinc, D. C. Ailion, B. Günther, and S. Žumer, Phys. Rev. Lett. **57**, 2826 (1986).
[11]See, for instance, R. Blinc and B. Žekš, *Soft Modes in Ferroelectrics and Antiferroelectrics* (North-Holland, Amsterdam, 1974).